Special Anniversary Issue: Professor Jan Czochralski Year 2013 — Invited Paper

High-Pressure Treatment up to 25 GPa of Czochralski Grown Si Samples Containing Different Admixtures and Defects

V.V. Shchennikov[a], Vs.V. Shchennikov[b], I.V. Korobeynikov[a,*] and N.V. Morozova[a]

[a]Institute of Metal Physics of Russian Academy of Sciences, Urals Division
18 S. Kovalevskaya Str.,Yekaterinburg 620990, Russia

[b]Institute of Engineering Sciences of Russian Academy of Sciences, Urals Division
34 Komsomolskaya Str., Yekaterinburg 620219, Russia

The thermoelectric properties of a set of single crystalline Si wafers with different oxygen concentration grown by the Czochralski technique have been studied at ultrahigh pressures up to 25 GPa. The dependence of semiconductor–metal transition pressure at Czochralski grown Si on the concentration c_O of the interstitial oxygen was found to present a convex curve with the maximum near $c_O \approx 9 \times 10^{17}$ cm^{-3}. The high pressure thermoelectric power method seems to be suitable for characterization of impurity-defect structure of Si wafers. For $Si_{1-x}Ge_x$ crystals ($1\% < x < 3\%$) the strong changes of both the value and the sign of thermoelectric power have been observed at pressures much less than ones of Si-I $\rightarrow$ Si-II transition. From nanoindentation data the phase transition Si-I $\rightarrow$ Si-II, corresponding to semiconductor–metal electronic transformation has been detected at the loading up to ≈ 10 mN. These findings suggest a way for creation of integrated circuits, in which zones with different types of conductivity and hence different p–n, p–n–p etc. structures may be "written" by applied stress at nanoscale level, and the control on the value of the above stresses now is possible by the proposed nanoindentation technique.

DOI: 10.12693/APhysPolA.124.244

PACS: 61.72.uf, 81.40.Vw, 72.20.Pa, 62.50.−p, 05.70.Fh

1. Introduction

Nowadays, in substrate manufacturing for advanced microelectronic devices and integrated circuits, silicon wafers are used, cut from single crystalline Si rods, grown typically by the Czochralski technique (Cz-Si) [1]. Silicon produced by this technique contains residual oxygen, located mostly in interstitial sites (O_i); this oxygen can affect electronic, mechanical, thermal, and other properties of Si wafers. Pre-annealing of Cz-Si at 570–770 K is known to form "thermal donors" connected with oxygen impurity. The energies of these donor states estimated using both Hall effect and deep-level transient spectroscopy (DLTS) correspond to $\approx$ 0.13–16 and 0.06–0.07 eV [2]. The above annealing is known to change the sign of conductivity of Cz-Si samples from p-type to n-type [3]. Above $\approx$ 820 K these thermal donors decay and in the temperature range $\approx$ 820–1170 K the generation of "new thermal donors" with the higher values of ionization energies occurs [2]. The origin of oxygen related "new donors" is related to oxygen precipitates [2, 3].

Annealing at high T generally tends to precipitation of oxygen interstitials with a creation of SiO_{2-x}, precipitates, precipitate–dislocation complexes, dislocations, and other defects. Electronic, mechanical, and optical properties of Cz-Si samples have been found to depend on the state of oxygen-defect system [2, 3]. In Refs. [4, 5] the measurements of thermoelectric power S (Seebeck effect) at high pressures P have been suggested for characterization of the oxygen-defect state of Cz-Si samples.

The results obtained on the Seebeck effect at high pressures for Cz-Si subjected to different P–T pre-treatments as well as doped by N impurity showed the dependence of both the sign of S and the total shape of $S(P)$ curve on the initial state of oxygen-impurity system; the pressure of phase transition from diamond-like to white tin-like lattice detected from $S(P)$ measurements being a function of oxygen content [5–7]. Pressure releasing leads to arising of metastable phases, $r8$ (Si-XII) below $\approx$ 8 GPa and $bc8$ (Si-III) below $\approx$ 2 GPa [8–12]. Si-III was found to be a p-type semimetal with a carrier concentration of $p \approx 10^{20}$ cm^{-3} [9, 12]. In Ref. [13] it was demonstrated that using stress-related techniques one can "write" conducting Si-III zones on silicon surface, and thus to create the semiconductor–metal structures. Recently at Cz-Si samples with small addition of Ge atoms (1.4–2.6%) the effect of switching of S sign found at low pressures [14] made it possible to create not only "semiconductor–metal" nanostructures, but also the various semiconductor p–n type structures at the samples surface. So, the investigation of the thermoelectric properties of Cz-Si under high pressures is of interest as for the characterization of the impurity-defect structure, as well as in the view of possible applications in microelectronics techniques.

In the present work results of high-pressure thermoelectrical investigations of Cz-Si with oxygen-related defects have been performed in a wide pressure range up to

*corresponding author; e-mail: i_korobeynikov@mail.ru, highpressgroup@mail.ru

$\approx$ 25 GPa, and then ones have been compared with especially processed nanoindentation data obtained on the same samples.

2. Experimental details

A quasi-hydrostatic pressure P was produced in the anvil-type sintered diamond chambers [15–17]. The samples for investigation were cut from the Si wafers in the form of plates with sizes ($\approx$ 200) $\times$ ($\approx$ 200) $\times$ ($\approx$ 20–50) μm^3 and were placed into a hole $\approx$ 250 μm in diameter drilled in the centre of a catlinite container (which served as a pressure-transmitting medium). Values of pressure were estimated with 10% uncertainty from a "stress-pressure" calibration curve obtained with assistance of known phase transitions in Bi, ZnS, GaP, etc. [15]. The high-pressure setup [17] made it possible to measure simultaneously several parameters: applied force, sample's contraction, anvils' temperatures, thermal difference ΔT along a sample, and electrical signal from a sample [16, 17]. A thermal difference was produced by heating of the anvils. The synthetic conducting diamond anvils served as a heater and a cooler in the S measurements [15]. A microindentation testing was carried out using a depth sensing Vickers microindenter, similar to the one described in Ref. [18] and Hysitron TI900 nanotester using Berkovich nanoindenter. Indentations were done at 5–10 points at the surface of the each sample.

Nowadays, the microindentation becomes a standard technique for testing of semiconductor single crystals, including silicon wafers [18, 19]. These measurements supply values of microhardness and Young's modulus as well [19]. Earlier Si and Ge were established to be the only semiconductors with microhardness values approximately coinciding at room temperature with the values $P_t \geq 10$ GPa of pressure-caused phase transitions into metallic phase with white-tin tetragonal lattice [20]. It was proved that the above phase transition indeed occurs under indenter tip [19–23]. So, we have chosen this technique for comparison with the high-pressure study in anvils cell.

TABLE

Properties of the P–T pre-treated Si samples.

No.	P–T pre-treatment			Concentration of interstitial oxygen c_O [$\times 10^{17}$ cm^{-3}]
	T [°C]	P [GPa]	t [h]	
1(I)	–	–	–	11.0
2(D1)	450	0.0001	10	10.3
3(D4)	450	1.4–1.45	10	7.7
4(C1)	650	0.0001	10	9.1
5(c70-I)	957	0.01	5	5.03
6(c70-II)	1130	1.2	5	8.27
7(c70-III)	560	0.0001	20	10.61
A01	–	0.0001	–	11.0–11.5
A02	450	0.0001	10	11.3
A03	450	0.0001	20	9.1
A04	450	0.0001	40	10

The interstitial oxygen concentration was determined by the Fourier transform infrared spectrometry (FTIR), using the conversion factor value equal to 2.45 $\times$ 10^{17} cm^{-3} (ASTM F 21-83 standard) [3]. The details are described in [3]. The properties of pre-treated Cz-Si samples are listed at Table. One can see that in the view of the pre-treatment performed the samples contain both thermal donors, as well as "new" thermal donors.

3. Results and discussion

P–T pre-treatment of the samples results in changing of both concentration and type of charge carriers due to formation of thermal donors [3] (Fig. 1). This leads to variation of $S(P)$ dependences for the samples measured (see Fig. 1). However, above the semiconductor–metal phase-transition point the behaviors of the $S(P)$ dependences for p- and n-type samples were rather similar (Fig. 1). The $S(P)$ dependence of the p-type sample firstly exhibited a minimum near 7–11 GPa, then the value of S increased to 13–14 GPa, and above 15–16 GPa S decreased again (Fig. 2). The last two features were also observed for n-type samples (Fig. 1b). Though the S values of all high-pressure metallic phases investigated were close to $S \approx 8 \pm 3$ μV/K, they changed abruptly with pressure, so the pressure derivative of S twice inverted its sign in the pressure range up to 20 GPa (Fig. 2). The sharp changes of $\mathrm{d}S/\mathrm{d}P$ may be related to the phase transformations (Fig. 2). However, the values of S of high-pressure metallic phases with a β-Sn structure and orthorhombic (above 12 GPa) and simple hexagonal (above 16 GPa) structures are approximately the same for different sample groups (Table).

At releasing of P the phase transitions in Si are known to happen at $\approx$ 9.4 GPa into rhombohedral phase Si-XII ($r8$) and at $\approx$ 2 GPa into Si-III ($bc8$) phase with body-centered cubic structure [9, 24]. By observing the changes in pressure coefficients of S with decreasing pressure below these values (Fig. 2) one can attribute ones to above phase transitions. S values of Si-III phase are larger than the ones of metallic phases, which agrees with Hall-effect data obtained after high-pressure treatment at $\approx$ 18 GPa [9]. According to the data [9], Si-III phase is a p-type semimetal with indirect band gap overlapping $\approx$ 0.3 eV and a carrier concentration of $n_p = (5 \pm 2) \times 10^{20}$ cm^{-3}. This conclusion is confirmed by the recent calculations of the electron band structure of Si-III phase [25] coinciding in general with previously published results [26, 27].

Annealing at high temperatures resulted in a non-monotonic decrease of the concentration of residual interstitial oxygen c_O in Cz-Si [3, 4]. The pressurized environment contributed to an additional decrease in c_O values (Table). In all sets of Cz-Si wafers, the regularity of the semiconductor–metal (S–M) phase transition pressure P_t on the concentration of residual interstitial oxygen c_O was evidenced (Fig. 3). Let us note that every point of Fig. 3 corresponds to particular pre-treatment conditions: temperature, time, pressure both for undoped and N-doped Cz-Si crystals. This dependence exhibits a maximum of P_t near $c_O \approx 9.10^{17}$ cm^{-3}

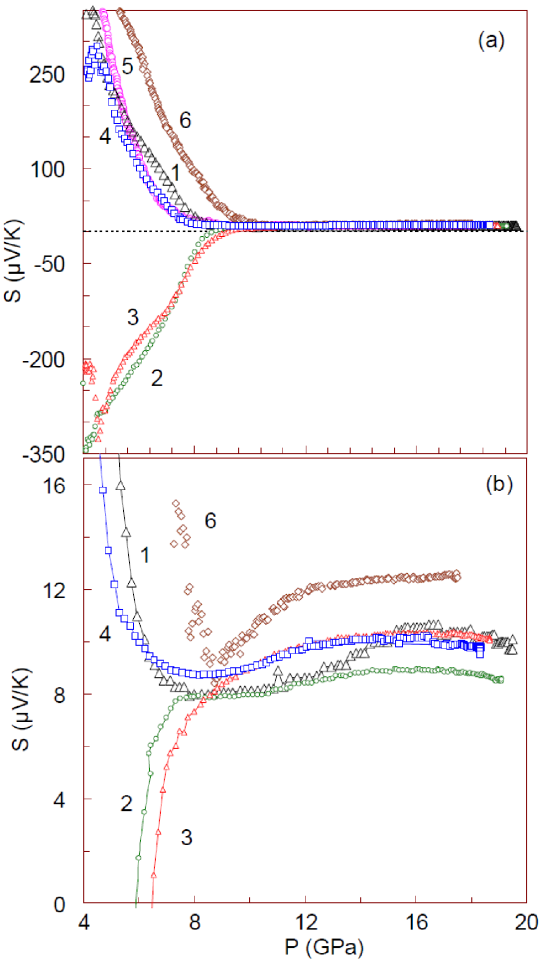

Fig. 1. (a) Dependence of thermopower on pressure for silicon samples with different pre-treatment conditions. The numbers near curves correspond to samples numbers in Table. (b) The same curves as in (a) in the reduced scale.

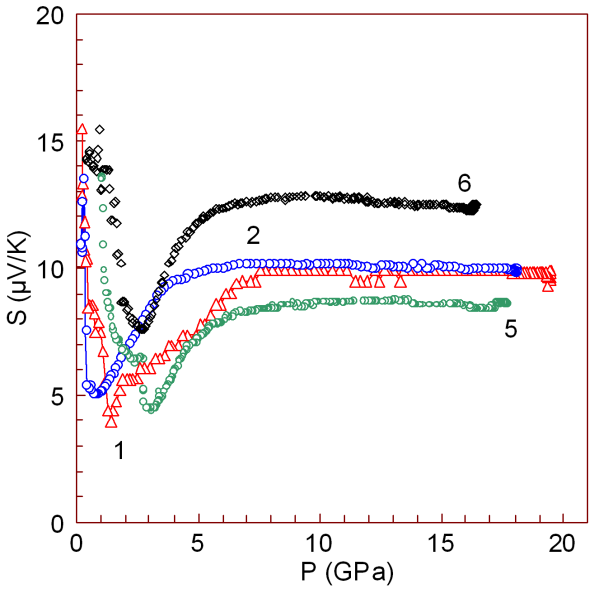

Fig. 2. Dependence of thermopower on pressure release for silicon samples with different pre-treatment conditions. The numbers near curves correspond to samples numbers in Table.

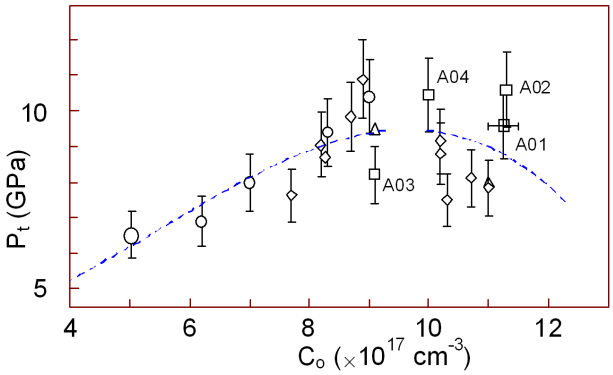

Fig. 3. Dependence of S–M phase transition pressure value P_t on concentration of interstitial oxygen for silicon samples with different pre-treatment conditions. Experimental data are taken from the present work (Fig. 1) as well as from [28]. The line is drawn as a guide for eyes.

probably related to the low concentration of nucleation sites for phase transitions. This has been offered as an explanation of the high value $P_t \approx 21$ GPa observed in Si nanocrystallites coated with a SiO_2 layer [29].

It needs to point out that the recording of the "beginning" of Si-I → Si-II phase transition (in fact — the corresponding S–M transition) depends on the technique used [24], e.g. X-ray data always relate to the completion of the transition, while the Raman data are sensitive both to the arising of small amount of new phase (precursor of transition), as well as to the conserving of negligible fraction of the initial one (after the completion of the transition) [30], and electrical resistivity data show the start of phase transition ahead of X-ray technique [24]. The variation of thermopower S at S–M phase transition always ought to pass ahead of resistivity changes (and vice versa at the reverse transition metal–semiconductor) due to relation between S, ρ, and thermal conductivity λ entities, derived for the first time in [31] for two-phase mixture with the variable configuration and concentration of semiconductor and metal phases

$$\frac{S - S_2}{S_1 - S_2} = \frac{\rho\lambda - \rho_2\lambda_2}{\rho_1\lambda_1 - \rho_2\lambda_2}. \qquad (1)$$

Here S_i, ρ_i, and λ_i ($i = 1, 2$) are the values of thermopower, electrical resistivity and thermal conductivity for semiconductor phase ($i = 1$) and high-pressure metallic phase ($i = 2$) [31].

With these reservations the $S(P)$ data may be considered for determination of the phase transition pressures P_t. The volumetric drops have been observed at

the Si-I → Si-II phase transition [4–7] accompanied by large volume contraction ≈ 20% [24] at pressures indeed somewhat larger than P_t obtained from $S(P)$ data [4–7].

The non-monotonic dependence of phase transition pressure P_t on the concentration of the interstitial oxygen may be explained using the similarity of P_t with the microhardness values H. For ternary semiconductor compounds the following dependence of H on the concentration of impurity (third component) is usually valid:

$$H(c) = (H_A - H_B)c + K(c)c(1-c), \quad (2)$$

tending always to the convex type of $H(c)$ curve as a function of the content [32]. Here H_A and H_B are values of H for A and B components, and K is a coefficient [32]. This hardening effect is due to the elastic interaction between solute atoms and screw dislocations [33, 34]. For correct calculations of microhardness dependence the equation is used taking into account the contribution in H of the stress field around solute atoms, caused by different size and modulus [32–34]:

$$\frac{dH}{d(x)^{0.5}} = 0.48G|\varepsilon_G - 6\gamma\varepsilon_a|, \quad (3)$$

with $\varepsilon_G = (dG/dx)/G$, $\varepsilon_a = (da/dx)/a$, G — the bulk shear modulus, a — the lattice constant and γ — the Grüneisen constant, and x — the content of the impurity (third component). Equation (3) confirms empirical convex type of H dependence for a lot of ternary semiconductor systems [32]. So, the similar dependence for P_t on the content of interstitial oxygen ought to be waiting. The dependence of P_t obtained from $S(P)$ data indeed may be described by the similar convex curve (Fig. 3).

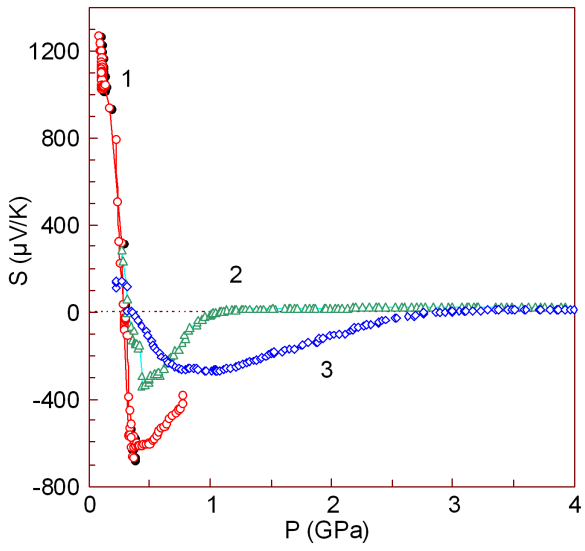

Fig. 4. Pressure dependences of thermopower of $Si_{1-x}Ge_x$ with x: 1 — 1.4%, 2 — 1.8% and 3 — 2.6%.

For the Cz-Si crystals with small amount of Ge atoms the results of $S(P)$ measurements strongly distinguish from ones for the above listed Ge-free Cz-Si samples (Fig. 4) [14]. The value of S suffers abrupt jumps with the sign inversion far from the expected structural phase transition Si-I → Si-II. The thermopower data show reversible p–n "switching" by applied pressure of ≈ 0.3–0.6 GPa [14] (Fig. 4). By application of higher pressures between 0.8 and 1.5 GPa, i.e., beyond the thermopower negative extremum point (Fig. 4) the irreversible p–n "switching" occurs [14]. Irreversible n–p turn to an almost compensated state with nearly equivalent p- and n-contributions in S is achieved by applied pressure above ≈ 2–3 GPa (Fig. 4). Germanium-doped Cz-Si with the amount of Ge exceeding ≈ 1% contains controlled strain in layered structures that tends to carriers mobility competitive with one for III–V semiconductors [35]. Ge atoms in Si are known to act as traps for donor-vacancy complexes [14, 36–39]. So, both the presences of Ge atoms, as well as the interstitial oxygen are responsible for such S "switching" effect [14]. This result discovered firstly at [14] made it possible to "write" the semiconductor zones with n- and p-type of conductivity at the surface of Ge-doped Cz-Si wafers, and thus to create semiconductor devices. The problem of creation of the controlled pressures at the small area of the wafer surface may be solved using nanoindentation technique.

Figure 5 demonstrates the phase transition recording during nanoindentation of the single crystalline Si-plate got with the nanomechanical instrument TI 900 Triboindenter using Berkovich triangle diamond indenter. The experimental data on nanoindentation have been subjected to mathematical treatment by the subtraction of nearly linear monotonic term according to the technique suggested in [7]. Several nanoindentation runs at different points of the sample surface reveal repeatability of the peak at load about 9 mN (samples No. 5 and No. 7). A small "dog-ear" at load of 10 mN for sample No. 6 also has reputability. That is why it also can be attributed to the beginning of phase transition at local area under tip of the indenter. The value of load corresponding to the phase transition Si-I → Si-II in Fig. 5 depends on the concentration of interstitial oxygen c_O in the same manner, as the value of transition pressure P_t recorded using $S(P)$ data (Figs. 1, 3). Thus, for the sample No. 6 the value of the load relevant to phase transition is higher than ones for samples No. 5 and 7 (Fig. 5) which correlates with the corresponding P_t data for these samples (Fig. 1b). According to the results of the present work (Fig. 3) and of the previously published papers [4–7] the p-type semimetal nanozones have to arise at the Si plate after the unloading. The recording of phase transition at Si at nanoindentation allows receiving the relation between the values of loading, on the one hand, and the values of pressure in the material near the indenter tip, on the other hand. The described above sharp drops of S with the sign inversion at Cz-Si(Ge) crystals may be obtained by nanoindentation technique, tending to possibility to "write" the semiconductor zones of n- and p-type at the Cz-Si based wafers surface similarly to the procedure decribed in [13].

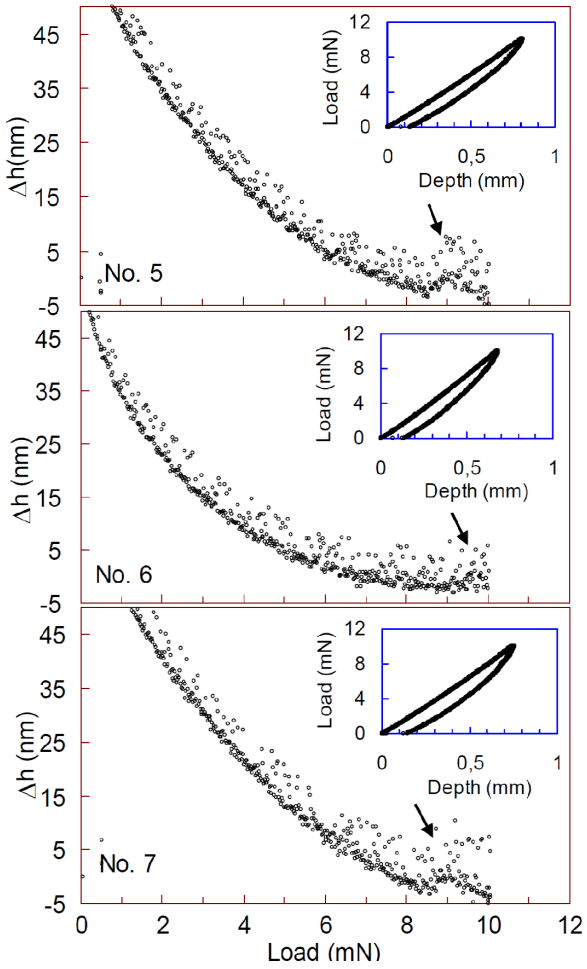

Fig. 5. Nanoindentation curves after subtracting of linear term for samples Nos. 5–6–7, Δh — a depth of indenter penetration after the subtraction of linear term. The arrow points the anomaly attributed to the S–M structural transition at about 9 mN of indenter loading (samples No. 5 and No. 7). At the figure for sample No. 6 there is a small "dog-ear" at load of 10 mN which may be attributed to the beginning of S–M transition. The insets show the initial shape of nanoindentation curves.

4. Conclusions

Thus, in the present work, the thermoelectric properties of a set of single crystal Si wafers with different oxygen concentration grown by the Czochralski technique have been studied at ultrahigh pressures up to 25 GPa. A shift was noticed of pressure P_t of the S–M phase transition to higher magnitudes for samples with intermediate oxygen concentrations. The shift was explained by the elevated mechanical strength and hardening of the crystals with oxygen-related defects. The correlation dependence of P_t on c_O discovered through all the sets of Si samples investigated was found to exhibit a maximum near $c_O \approx 9 \times 10^{17}$ cm^{-3}. The high-pressure thermoelectric power method [40, 41] seems to be suitable for characterization of Si wafers exposed to various pre-treatments [7]. Anomalies were observed also on the loading curves of nanoindentation in the vicinity of the S–M phase transition point. These findings suggest a way of functionality extension of Si-based devices for emergent applications. For instance, Si-based structures possessing the abrupt jumps of S under pressure-like Cz-Si:Ge samples [14] may be utilized for creation of integrated circuits, in which zones with different types of conductivity or different elements (p–n diodes, p–n memory elements) may be "written" by applied stress at nanoscale level, and the control on the value of the above stresses now is possible by the proposed nanoindentation technique.

Acknowledgments

The authors are grateful to Dr. A. Misiuk and Dr. N.V. Abrosimov for the samples given. The work is supported by UD RAS as part of Program "Matter at high energy densities" of the Presidium of RAS, project No. 12-P-2-1004, and by the Oriented Basic Research Project of the Ural Division of RAS, project No. 13-2-032-YaC.

References

[1] K. Nakai, Y. Inoue, H. Yokota, A. Ikari, J. Takahashi, A. Tachikawa, K. Kitahara, Y. Ohta, W. Ohashi, *J. Appl. Phys.* **89**, 4301 (2001).

[2] V.S Vavilov, A.R. Chelyadinskii, *Phys. Usp.* **38**, 333 (1995).

[3] A. Misiuk, W. Jung, B. Surma, J. Jun, M. Rozental, *Solid State Phenom.* **57-58**, 393 (1997).

[4] S.V. Ovsyannikov, V.V. Shchennikov, A. Misiuk, *JETP Lett.* **80**, 405 (2004).

[5] V.V. Shchennikov, S.V. Gudina, A. Misiuk, S.N. Shamin, *Physica B: Condens. Matter* **340-342**, 1026 (2003).

[6] V.V. Shchennikov, S.V. Ovsyannikov, A. Misiuk, Vs.V. Shchennikov Jr., *Phys. Status Solidi B* **241**, 3242 (2004).

[7] Vs.V. Shchennikov Jr, S.V. Ovsyannikov, V.V. Shchennikov, N.A. Shaidarova, A. Misiuk, S.V. Smirnov, D. Yang, *Mater. Sci. Eng. A* **462**, 347 (2007).

[8] R.H. Wentorf Jr., J.S. Kasper, *Science* **139**, 339 (1963).

[9] J.M. Besson, E.H. Mokhtari, J. Gonzalez, G. Weill, *Phys. Rev. Lett.* **59**, 473 (1987).

[10] M. Hanfland, K. Syassen, *High Press. Res.* **3**, 242 (1990).

[11] H. Olijnyk, A.P. Jephcoat, *Phys. Status Solidi B* **211**, 413 (1999).

[12] S.V. Ovsyannikov, V.V. Shchennikov, A. Misiuk, V.V. Shchennikov, Jr., *Solid State Commun.* **132**, 545 (2004).

[13] S. Ruffell, K. Sears, J.E. Bradby, J.S. Williams, *Appl. Phys. Lett.* **98**, 052105 (2011).

[14] S.V. Ovsyannikov, I.V. Korobeinikov, N.V. Morozova, A. Misiuk, N.V. Abrosimov, V.V. Shchennikov, *Appl. Phys. Lett.* **101**, 062107 (2012).

[15] I.M. Tsidil'kovskii, V.V. Shchennikov, N.G. Gluzman, *Sov. Phys. Semicond.* **17**, 604 (1983).

[16] V.V. Shchennikov, S.V. Popova, A. Misiuk, *Tech. Phys. Lett.* **29**, 598 (2003).

[17] S.V. Ovsyannikov, V.V. Shchennikov, Y.S. Ponosov, S.V. Gudina, V.G. Guk, E.P. Skipetrov, V.E. Mogilenskikh, *J. Phys. D, Appl. Phys.* **37**, 1151 (2004).

[18] F. Yang, P. Fei, *Semicond. Sci. Technol.* **19**, 1165 (2004).

[19] S.E. Grillo, M. Ducarroir, M. Nadal, E. Tournié, J.-P. Faurie, *J. Phys. D, Appl. Phys.* **36**, L5 (2003).

[20] I.V. Gridneva, Yu.V. Milman, V.I. Trefilov, *Phys. Status Solidi A* **14**, 177 (1972).

[21] V. Domnich, Yu. Gogotsi, S. Dub, *Appl. Phys. Lett.* **76**, 2214 (2000).

[22] V.G. Eremenko, V.I. Nikitenko, *Phys. Status Solidi A* **14**, 317 (1972).

[23] V.V. Shchennikov, S.V. Gudina, A. Misiuk, S.N. Shamin, S.V. Ovsyannikov, *Eur. Phys. J., Appl. Phys.* **27**, 145 (2004).

[24] A. Mujica, A. Rubio, A. Munoz, R.J. Needs, *Rev. Mod. Phys.* **75**, 863 (2003).

[25] V.V. Shchennikov, Vs.V. Shchennikov, S.V. Streltsov, I.V. Korobeynikov, S.V. Ovsyannikov, *J. Electron. Mater.* **42**, 2249 (2013).

[26] B.D. Malone, J.D. Sau, M.L. Cohen, *Phys. Rev. B* **78**, 035210 (2008).

[27] B.D. Malone, M.L. Cohen, *Phys. Rev. B* **85**, 024116 (2012).

[28] S.V. Ovsyannikov, V.V. Shchennikov Jr, N.A. Shaydarova, V.V. Shchennikov, A. Misiuk, D. Yang, I.V. Antonova, S.N. Shamin, *Physica B: Condens. Matter* **376-377**, 177 (2006).

[29] S.H. Tolbert, A.B. Herhold, L.E. Brus, A.P. Alivisatos, *Phys. Rev. Lett.* **76**, 4384 (1996).

[30] S. Ves, Yu.A. Pusep, K. Syassen, M. Cardona, *Solid State Commun.* **70**, 257 (1989).

[31] V.V. Shchennikov, *Fiz. Met. Metalloved.* **67**, 93 (1989).

[32] V.V. Shchennikov, S.V. Ovsyannikov, N.Yu. Frolova, *J. Phys. D, Appl. Phys.* **36**, 2021 (2003).

[33] A. Fissel, M. Schenk, A. Engel, *Cryst. Res. Technol.* **24**, 557 (1989).

[34] A. Fissel, M. Schenk, *Cryst. Res. Technol.* **25**, 89 (1990).

[35] A. Misiuk, B. Surma, A. Wnuk, J. Bak-Misiuk, P. Romanowski, W. Wierzchowski, K. Wieteska, N. Abrosimov, W. Graeff, *Acta Crystallogr. A* **64**, C441 (2008).

[36] V.P. Markevich, A.R. Peaker, L.I. Murin, N.V. Abrosimov, *Appl. Phys. Lett.* **82**, 2652 (2003).

[37] A. Misiuk, N.V. Abrosimov, P. Romanowski, J. Bak-Misiuk, A. Wnuk, B. Surma, W. Wierzchowski, K. Wieteska, W. Graeff, M. Prujszczyk, *Mater. Sci. Eng. B* **154-155**, 137 (2008).

[38] J. Coutinho, F. Castro, V.J.B. Torres, A. Carvalho, M. Barroso, P.R. Briddon, *Thin Solid Films* **518**, 2381 (2010).

[39] M. Arivanandhan, R. Gotoh, T. Watahiki, K. Fujiwara, Y. Hayakawa, S. Uda, M. Konagai, *J. Appl. Phys.* **111**, 043707 (2012).

[40] V.V. Shchennikov, S.V. Ovsyannikov, *JETP Lett.* **84**, 21 (2006).

[41] V.V. Shchennikov, S.V. Ovsyannikov, A.Y. Derevskov, V.V. Shchennikov Jr., *J. Phys. Chem. Solids* **67**, 2203 (2006).